View metadata, citation and similar papers at core.ac.uk

brought to you by CORE

provided by Elsevier - Publisher Connector

Arabian Journal of Chemistry (2016) xxx, xxx–xxx

King Saud University

Arabian Journal of Chemistry

www.ksu.edu.sa
www.sciencedirect.com

ORIGINAL ARTICLE

Removal of lead from aqueous solutions by ferric activated sludge-based adsorbent derived from biological sludge

Xin Yang, Guoren Xu *, Huarong Yu

State Key Laboratory of Urban Water Resource and Environment, Harbin Institute of Technology, Harbin 150090, China

Received 26 January 2016; accepted 25 April 2016

KEYWORDS

Biological sludge;
Ferric activation;
Pyrolysis;
Sludge-based adsorbent;
Adsorption;
Heavy metal

Abstract Ferric activation was novelly used to prepare sludge-based adsorbent (SBA) through pyrolysis treatment of biological sludge, and the adsorbents were applied to adsorb Pb^{2+} ions from aqueous solution. The ferric-activated SBA showed a favorable porous structure development and enhanced Pb^{2+} ions removal, with the maximum sorption capacity of 42.96 mg/g. The optimum adsorption was observed in a wide pH range of 4–6. The adsorption data fitted the Freundlich model well, indicating heterogeneous lead coverage on the adsorbents. Pseudo-second order model validated the kinetic data, suggesting that the rate-limiting step of the adsorption process was chemical sorption. The mechanism of Pb^{2+} ions removal involved ion exchange, precipitation, and surface complexation. The higher adsorption of ferric-activated SBA was due to the enhancive surface area that provided a larger number of active sites for adsorbate, the precipitation, and the formation of the surface complex Fe—OPb^{2+}. The results demonstrate that ferric-activated SBA can be used as an effective adsorbent for Pb^{2+} ions removal from aqueous solution, which will also provide an option for sludge valorization.

© 2016 Production and hosting by Elsevier B.V. on behalf of King Saud University. This is an open access article under the CC BY-NC-ND license (http://creativecommons.org/licenses/by-nc-nd/4.0/).

1. Introduction

Lead is a priority pollutant, widely used in many industrial activities such as mining, smelting, petroleum refining, printing, pigment production, and battery manufacturing. Water pollution caused by lead has become a serious problem for environment and public health. Metals are non-biodegradable and tend to accumulate in living organisms (Ge et al., 2012; Sud et al., 2008), and it is therefore necessary to remove lead from wastewaters before releasing into the environment.

Conventional techniques for removing Pb^{2+} ions from aqueous phases include chemical precipitation, ion exchange, biological treatment, membrane filtration, electrochemical treatment, and adsorption (Nguyen et al., 2013; Zhu et al., 2014). Among them, adsorption is regarded as a simple, effective, and economical method (Ihsanullah et al., 2016). The utilization of low-cost and effective adsorbents is crucial in adsorption.

Sewage sludge is a by-product of municipal wastewater treatment, containing amounts of organic pollutants, pathogens and heavy metals. Owing to the high contents of organic substances, sludge has been

* Corresponding author. Tel./fax: +86 0451 86282559.
E-mail address: xgr@hit.edu.cn (G. Xu).

Peer review under responsibility of King Saud University.

ELSEVIER Production and hosting by Elsevier

http://dx.doi.org/10.1016/j.arabjc.2016.04.017
1878-5352 © 2016 Production and hosting by Elsevier B.V. on behalf of King Saud University.
This is an open access article under the CC BY-NC-ND license (http://creativecommons.org/licenses/by-nc-nd/4.0/).

Please cite this article in press as: Yang, X. et al., Removal of lead from aqueous solutions by ferric activated sludge-based adsorbent derived from biological sludge. Arabian Journal of Chemistry (2016), http://dx.doi.org/10.1016/j.arabjc.2016.04.017

proposed as a suitable low-cost raw material for the production of activated carbon through pyrolysis (Hadi et al., 2015; Zielińska and Oleszczuk, 2015). The porous carbonaceous material can be used to adsorb heavy metals, antibiotics, dyes, and other organic pollutants from aqueous solutions (Ahmed et al., 2016; Xu et al., 2015). Thermal treatment can embed heavy metals into solid matrix to improve the stability of metals (Chen et al., 2014; Xu et al., 2015), and reduce the environmental risks caused by the metal leaching toxicity. The pyrolytic conversion of sludge into sludge-based adsorbent (SBA) is a promising option to disposal this waste, and turn low-cost solid waste into useful material for wastewater treatment.

In the preparation of SBA, chemical activation is employed, which could affect the pore structure, functional groups and metal adsorption performance of SBA (Jin et al., 2014; Trakal et al., 2014). The commonly used chemical activators are $ZnCl_2$, NaOH, KOH, H_2SO_4 and H_3PO_4 (Hadi et al., 2015). Pan et al. (2011) reported that SBA made from chemical sludge had a higher surface area and adsorption capacity for pollutants than that produced from biological sludge. Chemical sludge is different from biological sludge, which generated from chemical precipitation of wastewater with coagulants. The presence of coagulants (e.g., ferric salts) and its by-product in chemical sludge may influence the textural properties of sludge derived adsorbents, and results in the promoted contaminants removal (Pan et al., 2011; Xu et al., 2005). According to our previous study (Yang et al., 2016), ferric activation has proved to be a novel and effective method for improving the porous structure development of SBA. However, there is little information on the application of ferric-activated SBA in Pb^{2+} ions removal, and its mechanisms responsible for Pb^{2+} sorption.

This study is aimed at evaluating the potential of SBA prepared from biological sludge through ferric activation for lead removal. The adsorbents prepared with and without ferric activation were compared for their physicochemical properties and adsorption capacity. The effects of pH, contact time, and initial Pb^{2+} concentration on the removal of Pb^{2+} ions were studied, in order to understand the kinetics and equilibrium of the process. Moreover, characterization of adsorbents before and after lead adsorption was analyzed using Fourier-transform infrared spectrometer (FTIR) and X-ray diffraction (XRD). The release of alkali (K^+ and Na^+) and alkaline-earth (Ca^{2+} and Mg^{2+}) metals after adsorption was also examined.

2. Experimental

2.1. Material and chemicals

Raw sludge was collected from a municipal wastewater treatment plant in Beijing, China, where wastewater employed an activated sludge biological treatment. The sludge was air-dried to constant weight, and ground into sizes below 1 mm. Ferric sulfate and lead nitrate were obtained from Tianjin Benchmark Chemical Reagent Co., Ltd. (Tianjin, China). A stock solution (1000 mg-Pb/L) was prepared by lead nitrate ($Pb(NO_3)_2$), and working solutions of various concentrations were diluted from the stock solution with deionized water. All laboratory wares were soaked in dilute nitric acid (10%) for at least 12 h, thoroughly flushed with tap water, and washed three times with deionized water. All chemicals were of analytical grade, and used as received.

2.2. Preparation of adsorbents

Raw sludge, and mixture of dried sludge and ferric sulfate at a 10:3 weight ratio were pyrolyzed (750 °C, 2 h) in a quartz-tube resistance furnace under an oxygen-deficient atmosphere. After cooling, the products were milled and sieved to 200 mesh. The adsorbents produced with and without ferric activation are referred to as ferric-activated SBA and SBA, respectively.

2.3. Characterization of the raw sludge and adsorbents

Element C, H, O, S and N contents in the raw sludge and adsorbents were determined by a Vario EL cube element analyzer (Elementar, Hanau, Germany) with a detection limit of 0.1%. The metal contents of samples were performed by X-ray fluorescence spectrometer (XRF; Axios PW4400, PANalytical acquires Claisse Inc., Netherlands). The textural properties were studied by physical adsorption of N_2 at −196 °C on a surface area analyzer (ASAP 2020M, Micromeritics Instrument Co., Norcross, GA, USA). The samples were outgassed overnight at 80 °C under vacuum prior to adsorption measurements. The specific surface area was estimated using the Brunauer–Emmett–Teller equation (Brunauer et al., 1938). The micropore volume (V_{mi}) was calculated by the t-plot method. The macropore volume, mesopore volume, and pore size distribution were obtained by the Barrette–Joynere–Halenda (BJH) method (Barrett et al., 1951).

The surface functional groups of adsorbents were examined by Fourier transform infrared (FTIR) spectroscope on a SPECTRUM ONE B instrument (PerkinElmer, Waltham, USA) in the 400–4000 cm^{-1} region. Powder X-ray diffraction (XRD) patterns of adsorbents were recorded using a Bruker D8 Advance X-ray diffractometer (Germany) with Cu Kα irradiation (40 kV, 40 mA). The Pb-loaded adsorbents were collected, washed with deionized water, and freeze-dried before FTIR and XRD analysis.

The point of zero charge (pH_{pzc}) was measured by the pH drift method (Babić et al., 1999; Li et al., 2012). Samples (about 0.1 g) were suspended in 0.1 M KNO_3 (50 mL). The suspension was adjusted to pH between 2 and 12 by 0.1 M HNO_3 or NaOH. After 48 h, the final pH of the solution was determined, and the pH at which final pH equals initial pH was taken as the pH_{pzc} of the tested sorbent.

2.4. Batch adsorption experiments

Batch experiments were conducted by mixing weighed amounts (5–80 mg) of the adsorbents with 50 mL of 50 mg/L $Pb(NO_3)_2$ solution (pH 5). Each mixture was shaken at 160 rpm at 25 °C for 24 h. After equilibrium, solutions were filtered through 0.45 μm microporous membranes, and the residual concentrations were determined using inductively coupled plasma optical emission spectroscopy (ICP-OES; Optima ICP 5300DV, Perkin–Elmer, USA). Using this batch experiment approach, the adsorption capacity of adsorbents was investigated over a pH range of 2.0–6.0. Kinetic studies were performed by adding 0.06 g of adsorbent in 50 mL $Pb(NO_3)_2$ solution with an initial concentration of 50 mg/L (pH 5.0). The adsorption time varied from 5 to 300 min.

The released alkali and alkaline earth metals (i.e., Ca^{2+}, Mg^{2+}, K^+, and Na^+) from the original adsorbents in the supernatant (pH 5) were measured by ICP-OES. The corresponding releases of Ca^{2+}, Mg^{2+}, K^+, and Na^+ from adsorbents with deionized water at pH 5 were also determined as blanks. The experiments were performed in triplicate.

Please cite this article in press as: Yang, X. et al., Removal of lead from aqueous solutions by ferric activated sludge-based adsorbent derived from biological sludge. Arabian Journal of Chemistry (2016), http://dx.doi.org/10.1016/j.arabjc.2016.04.017

The removal efficiency and adsorption capacity of adsorbents were calculated as follows:

$$\text{The removal efficiency } (\%) = 100(C_0 - C_e)/C_0 \quad (1)$$

$$\text{The adsorption capacity } q_e = (C_0 - C_e)V/W \quad (2)$$

where C_0 and C_e (mg/L) are the initial and equilibrium concentrations of Pb^{2+} ions, respectively. V (L) is the solution volume, and W (g) is the adsorbent weight.

2.4.1. Adsorption kinetics

The experimental adsorption data were analyzed by Pseudo-first order and Pseudo-second order kinetic models (Velghe et al., 2012):

$$\text{Pseudo-first order model } q_t = q_e(1 - e^{-K_1 t}) \quad (3)$$

$$\text{Pseudo-second order model } q_t = K_2 q_e^2 t/(1 + K_2 q_e t) \quad (4)$$

where q_e (mg/g) and q_t (mg/g) are the amount of Pb^{2+} adsorbed per unit weight of adsorbent at equilibrium and time t (min), respectively; K_1 (min^{-1}) and K_2 [g/(mg min)] are the adsorption rate constants of Pseudo-first order and Pseudo-second order models, respectively.

2.4.2. Adsorption isotherm

Langmuir and Freundlich isotherm models were used to applied to fit the adsorption data as follows (Liu et al., 2010):

$$\text{The Langmuir model } q_e = q_m K_L C_e/(1 + K_L C_e) \quad (5)$$

$$\text{The Freundlich model } q_e = K_F C_e^{1/n} \quad (6)$$

where q_m (mg/g) and K_L (L/mg) are Langmuir constants related to adsorption capacity and energy, respectively; K_F (mg/g) and n are Freundlich constants associated with the sorption capacity and intensity, respectively.

The essential characteristic of the Langmuir equation can be expressed by a dimensionless constant, the equilibrium parameter (R_L):

$$\text{The Langmuir equilibrium parameter } R_L = 1/(1 + K_L C_0) \quad (7)$$

The value of R_L suggests the isotherm type to be irreversible ($R_L = 0$), favorable ($0 < R_L < 1$), linear ($R_L = 1$), or unfavorable ($R_L > 1$) (Zhu et al., 2013).

3. Results and discussion

3.1. Characterization of raw sludge and adsorbents

The properties of the raw sludge and adsorbents, containing pH_{pzc} and elemental composition, are presented in Table 1 (Yang et al., 2016). The relative elemental contents of C, H, O and N in the adsorbents decreased, compared to the raw sludge. The reduction was because that the loss of volatile matters took away amount of surface functional group elements (C, H, O and N) during the pyrolysis process (Rio et al., 2005). The data in Table 1 show that the pH_{pzc} of the raw sludge increased from 6.33 to around 8.0 after thermal treatment, which was due to the polymerization/condensation reactions and the release of acidic surface groups (Méndez et al., 2013).

Table 1 Main properties of the raw sludge and adsorbents.

	Raw sludge	SBA	Ferric-activated SBA
pH_{pzc}	6.33	8.14	8.03
Pyrolysis yield (%)	–	40.53	41.29
Ultimate analysis (%)			
C	37.48	30.38	26.06
H	5.83	0.92	1.02
O	21.44	12.02	14.91
N	6.69	1.58	1.90
S	1.86	0.39	9.76
P	5.25	13.08	6.17
Metal content (%)			
Na	0.23	0.71	0.49
Mg	1.07	3.02	1.63
Al	1.60	4.84	2.69
Si	4.41	13.73	7.44
K	2.71	5.85	2.73
Ca	3.90	8.15	3.74
Ti	0.25	0.52	0.22
Mn	0.03	0.08	0.05
Fe	2.83	5.33	22.55
Cu	0.06	0.09	0.04
Zn	0.25	0.38	0.18

The textural parameters of the raw sludge and adsorbents are summarized in Table 2 (Yang et al., 2016). It was noticed that the surface area of ferric-activated SBA was 100.48 m^2/g, which was more than 43 times that of pristine SBA. The pore volumes of SBA and ferric-activated SBA were 0.010 and 0.139 cm^3/g, respectively, and the micropore volumes varied in the range $(0.0061–1.797) \times 10^{-2}$ cm^3/g. This result implied that the increase in pore volume after ferric activation was mainly related to the increase in mesopores and macropores. The average pore size of raw sludge and adsorbents were all in the range of 2–50 nm, indicating that they were mesoporous materials.

As shown in Table 2, ferric-activated SBA exhibited greater mesoporosity development degrees than feedstock and SBA. The existence of ferric activator would boost the fragmentation of sludge organic compounds, causing a gradual reorganization of the solid matrix and the porous structure development (Yang et al., 2016). The reaction between ferric activator and sludge could produce iron compounds and other by-products, which might occur in the immediate area of the metal particles (Kacan, 2016), leading to the formation of mesopores by holes intercalated into the solid matrix (Liu et al., 2010).

Table 2 Textural properties of raw sludge and adsorbents.

Samples	Specific surface area (m^2/g)		Pore volume (cm^3/g)		D_p (nm)	$\frac{V_{mes}}{V_t}$ (%)
	BET method	Langmuir method	V_t	V_i		
Raw sludge	1.50	1.93	0.013	0.00057	10.13	95.65
SBA	2.33	3.27	0.010	0.00006	8.54	99.36
Ferric-activated SBA	100.48	136.72	0.139	0.018	4.46	87.03

V_t: total pore volume; V_i: micropore volumes; D_p: average pore size; V_{mes}: mesopore volumes.

Please cite this article in press as: Yang, X. et al., Removal of lead from aqueous solutions by ferric activated sludge-based adsorbent derived from biological sludge. Arabian Journal of Chemistry (2016), http://dx.doi.org/10.1016/j.arabjc.2016.04.017

3.2. Adsorption studies

3.2.1. Effect of pH

The effect of pH on Pb^{2+} adsorption by SBA and ferric-activated SBA is shown in Fig. 1a. The Pb^{2+} removal increased rapidly as the initial pH increased from 2.0 to 5.0, and then remained constant (Fig. 1a). The low uptake of Pb^{2+} in an acidic medium was attributed to the high concentration of H^+ ions, which competed for the available binding sites on the adsorbents surface (Badruddoza et al., 2013). The pH_{pzc} values of SBA and ferric-activated SBA were both around 8.0 (Table 1), indicating that the adsorbents had positive surface charges under the test conditions. As the solution pH decreased, the electrostatic repulsion between the positively-charged Pb^{2+} and adsorbents increased, leading to the decline of removal efficiency. At pH 5.0, the Pb^{2+} removal of SBA and ferric-activated SBA was 89.89% and 98.46%, respectively. Ferric activation could facilitate the development of a porous structure and the formation of iron compounds in the solid products, as discussed in our previous study (Yang et al., 2016). The promoted physical and chemical properties of ferric-activated adsorbent, leading to the increase in Pb^{2+} ions adsorption.

Lead exhibits different species, depending on the pH (Fig. 1b). When the solution pH exceeds 6, the amount of soluble Pb decreases sharply; as the pH value reaches 9, soluble Pb^{2+} ions disappear almost completely in the solution. Previous studies have shown that Pb^{2+} ions are precipitated due to the formation of lead hydroxide at pH > 6.0 (Elaigwu et al., 2014; Lu et al., 2012; Mohan et al., 2014). From Fig. 1a, when the initial pH was 5.0, the corresponding equilibrium pH values of SBA and ferric-activated SBA were both greater than 6.0, indicating that the mechanism of lead removal involved adsorption and precipitation.

Because of the competitive adsorption of H^+ and Pb^{2+} at low pH and the formation of lead precipitates at high pH, the optimum initial pH for Pb^{2+} ion adsorption on the SBA and ferric-activated SBA was 5.0. Similar results, using other adsorbents, were reported in the literature (Karami, 2013; Nguyen et al., 2013).

3.2.2. Adsorption kinetics

Kinetic investigations showed that the Pb^{2+} adsorption on the SBA and ferric-activated SBA were quick initially, and then decreased with increasing contact time until an equilibrium was reached (Fig. 2). For the ferric-activated SBA, a rapid increase was observed within the first 60 min, and equilibrium for Pb^{2+} adsorption was reached in 3 h. In the case of SBA, Pb^{2+} adsorption equilibrium was achieved at 5 h. Under the test conditions, the adsorption capacity of ferric-activated SBA was higher than that of non-activated SBA over time, indicating the better adsorption property of ferric-activated SBA to Pb^{2+} ions.

Pseudo-first order and Pseudo-second order models were employed to investigate the adsorption processes. The adsorption kinetics parameters are shown in Tables 3. The second order correlation coefficients was superior to the first order coefficients, and the values of $q_{e,cal}$ showed good agreement with those of $q_{e,exp}$. These results indicated that the experimental data fitted well to the Pseudo-second order model, and chemisorption was the rate-determining step in the lead adsorption (Velghe et al., 2012; Wang et al., 2010). Compared with SBA, the ferric-activated SBA showed a higher k_2 value (0.655 vs 0.246), suggesting the faster Pb^{2+} adsorption rate of ferric-activated SBA.

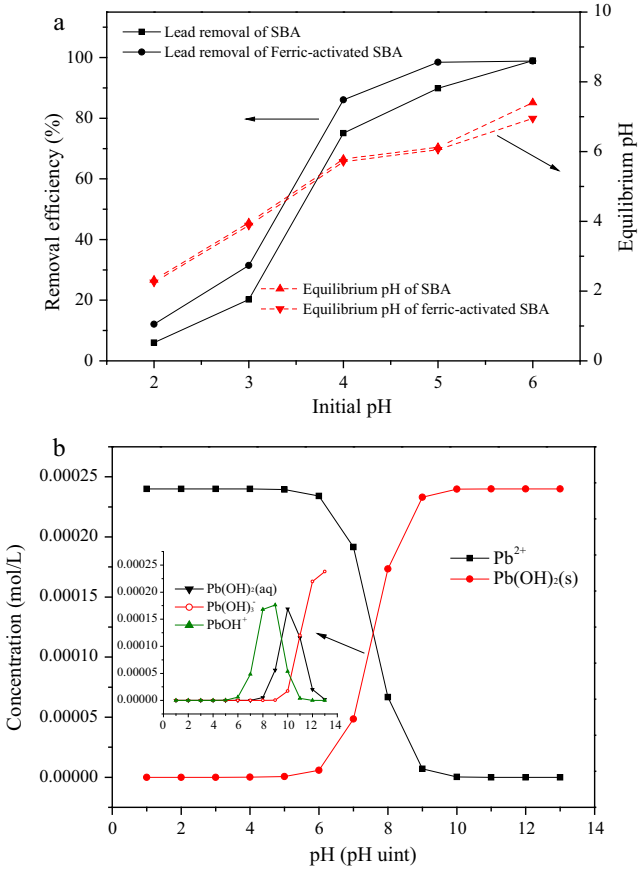

Figure 1 Effect of pH on adsorption of Pb^{2+} ions (a), speciation of Pb in aqueous solutions as a function of pH (b), and simulation using Visual MINTEQ ver. 3.0 [pH ranges from 1 to 13 pH unit; and the total Pb concentration is 0.24 mmol/L (50 mg/L)].

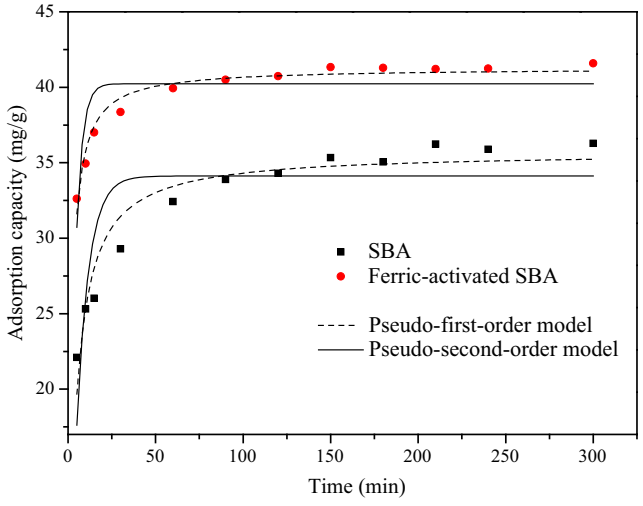

Figure 2 Adsorption kinetics of Pb^{2+} ions on adsorbents.

Table 3 Kinetics parameters of Pseudo-first-order and Pseudo-second-order models for adsorption of Pb^{2+} ions on adsorbents.

Samples	$q_{e,exp}$ (mg/g)	Pseudo-first-order model			Pseudo-second-order model		
		$q_{e,cal}$ (mg/g)	k_1 (min^{-1})	R^2	$q_{e,cal}$ (mg/g)	k_2 (g mg^{-1} min^{-1})	R^2
SBA	36.55	33.12	0.145	0.888	35.71	0.246	0.920
Ferric-activated SBA	42.96	38.23	0.289	0.749	41.28	0.655	0.958

As illustrated in Table 3, the equilibrium sorption capacity of ferric-activated SBA was 42.96 mg/g. This value is comparable with those of previous researches using adsorbents derived from waste resources, e.g., 30.88 mg/g for sewage sludge (Lu et al., 2012), 7.40 mg/g for *Prosopis africana* shell (Elaigwu et al., 2014), and 10.38 mg/g for oak bark (Mohan et al., 2014).

3.2.3. Adsorption isotherms

The adsorption isotherms for Pb^{2+} adsorption by adsorbents are presented in Fig. 3, and the isotherm parameters for fitting the Langmuir and Freundlich isotherm models are summarized in Table 4. The adsorption capacity of ferric-activated SBA was higher than that of non-activated SBA (Fig. 3), suggesting the stronger affinity of ferric-activated SBA for Pb^{2+} ions.

As shown in Table 4, Freundlich model fitted the equilibrium data better than the Langmuir model, with the correlation coefficients (R^2) higher than 0.97, indicating heterogeneous lead coverage of the adsorbents. Similar result was also reported by Lu et al. (2012); they used sewage sludge-derived biochar to adsorb Pb^{2+} ions. The K_F value of ferric-activated SBA was larger than that of SBA, indicating the higher adsorption capacity of ferric-activated SBA. The Freundlich parameters, $1/n$ values, were less than 1, denoting favorable adsorption of Pb^{2+} ions by the adsorbents. The dimensionless constants R_L fell within the range 0 and 1 (Table 4), which also suggested that the Pb^{2+} ions adsorption onto the adsorbents was favorable.

Based on the analysis of adsorption isotherms and kinetics, the experimental data were well described by Freundlich model and Pseudo-second order model. These results denoted that the adsorption of Pb^{2+} ions from aqueous solutions formed a heterogeneous cover over the adsorbents surface mainly through chemical adsorption phenomena (Velghe et al., 2012).

Table 4 Isotherm parameters for adsorption of Pb^{2+} ions on adsorbents at 25 °C.

Samples	Langmuir				Freundlich		
	q_m (mg/g)	K_L (L/mg)	R_L	R^2	K_F (mg/g)	$1/n$	R^2
SBA	33.41	44.24	0.0004	0.760	30.26	0.0333	0.970
Ferric-activated SBA	42.98	8.94	0.0022	0.736	35.33	0.0659	0.988

3.3. Desorption

In practical applications, desorption and sorbent regeneration are important properties of the adsorbent. As shown in Fig. 4, the desorption rate of different eluents for the Pb-loaded adsorbents decreased in the order HNO_3 > EDTA > deionized water. Due to the abundant H^+ ions in the solution, a dominant protonation reaction could occur between H^+ ions and active sites (Yu et al., 2013). Therefore, the complexation between the active sites and metal ions was prevented, and the lead precipitate dissolved. In terms of HNO_3, the desorption rates of SBA and ferric-activated SBA were greater than 85%. The result suggested that 0.1 M HNO_3 was suitable for desorbing Pb^{2+} ions from the adsorbents. After desorption, the adsorbents can be mixed with raw sludge to re-prepare sludge derived adsorbent.

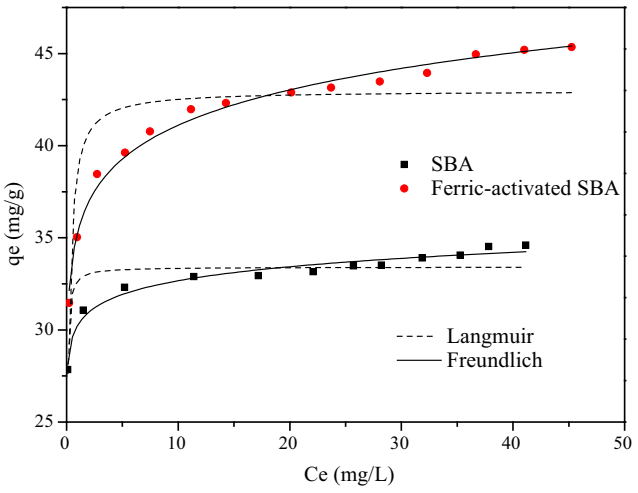

Figure 3 Adsorption isotherms of Pb^{2+} ions on adsorbents.

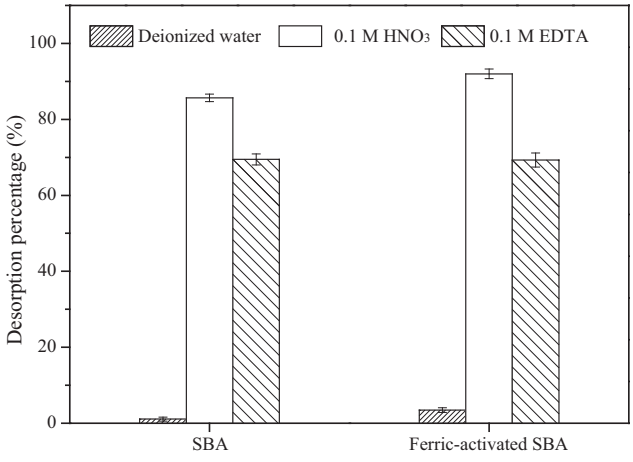

Figure 4 Desorption rates of Pb-loaded adsorbents.

3.4. Mechanisms of Pb^{2+} ion removal

Understanding adsorption mechanisms is essential to investigate the influence of ferric activation on the lead adsorption, and to achieve effective removal of Pb^{2+} ions from aqueous solutions. The mechanisms of Pb^{2+} adsorption on the adsorbents can be classified into three categories: (i) ion exchange; (ii) precipitation on the surface; and (iii) surface complexation.

Mechanism I:

Research suggested that an ion-exchange mechanism occurred between sludge-derived biochar and metal ions (Lu et al., 2012). The mechanism of Pb^{2+} ion removal by the adsorbents was investigated by determining the release of alkali (K^+ and Na^+) and alkaline-earth (Ca^{2+} and Mg^{2+}) metals after lead removal. The net release of Ca^{2+}, Mg^{2+}, K^+ and Na^+ was calculated by subtracting the amount released when adsorbents was mixed with deionized water (pH 5) from the amount of these cations released in the supernatant at equilibrium. For SBA and ferric-activated SBA, the total concentrations of released cations (Ca^{2+}, Mg^{2+}, ½ K^+, and ½ Na^+) were 13.89% and 22.09%, respectively, of the relevant total lead removal at initial pH 5 (Table 5). These results indicated the involvement of ion exchange during the removal of Pb^{2+} ions by adsorbents, monovalent and divalent cation releasing from the mineral matrix and the site replaced by Pb^{2+} forming new bond (Iqbal et al., 2009). However, the total amount of cations released was lower than the amount of Pb^{2+} captured, denoting that other mechanisms were also responsible for Pb^{2+} removal.

Mechanism II:

The XRD patterns of adsorbents before and after Pb^{2+} adsorption are shown in Fig. 5. Quartz and dolomite were the main crystalline phases in the adsorbents. Compared with SBA, the iron compounds of Fe_2O_3 and iron sulfide (FeS or $Fe_{1-x}S$, $x < 1$) were identified in ferric-activated SBA (Fig. 5). During the thermal treatment process, $Fe_{1-x}S$, and FeS were created by the reaction of ferric activator [$Fe_2(SO_4)_3$] under the reductive atmosphere provided by sludge pyrolysis, and Fe_2O_3 was generated from the activator self-decomposition (Yang et al., 2016).

From Fig. 5, the XRD patterns showed new peaks of crystalline $Pb_3(CO_3)_2(OH)_2$ (hydrocerussite) and Pb_2SiO_4 in the SBA after adsorption. The $Pb_3(CO_3)_2(OH)_2$ formation can be described as follows (Cao et al., 2009):

$$2HCO_3^- + 3Pb^{2+} + 4OH^- \rightarrow Pb_3(CO_3)_2(OH)_2 + 2H_2O \quad (8)$$

The greater increase in the amount of soluble Mg after adsorption with SBA (Table 5), may be due to dissolution of some Mg-substituted calcite (Cao and Harris, 2010), providing more carbonate for hydrocerussite precipitation. The precipitation of lead silicate was possibly attributed to reactions between Pb and activated silica on the SBA, because abundant amounts of activated silica were presented in the original SBA (Table 1). The Pb–Si precipitation was also reported by Lu et al. (2012).

The XRD data of ferric-activated SBA after metal adsorption, show peaks of lanarkite ($Pb(SO_4)\cdot PbO$), indicating a possible formation of lead sulfur precipitation. As shown in Table 1, the elemental contents of S in the adsorbents increased from 0.39% to 9.76% after activation with ferric sulfate, which might contribute to the formation of Pb–S precipitates. Research by Wang et al. (2015) showed that the precipitation could occur between Pb^{2+} ions and the S-containing substances in the adsorbents, and form the precipitates of $Pb_2(SO_4)O$.

Some other Pb precipitates, such as $Pb(OH)_2$, $Pb_9(PO_4)_6$, $5PbO\cdot P_2O_5\cdot SiO_2$, and PbS have also been reported in previous studies (Cao et al., 2009; Hien Hoa et al., 2007; Lu et al., 2012). In this study, the main precipitates of SBA were $Pb_3(CO_3)_2(OH)_2$ and Pb_2SiO_4, and $Pb(SO_4)\cdot PbO$ was the major precipitate of ferric-activated SBA. The precipitation would contribute to the removal of Pb^{2+} ions from solution by SBA and ferric activated SBA.

Mechanism III:

The FTIR spectra of native and Pb-loaded adsorbents are shown in Fig. 6. The broad band at around 1600–1540 cm^{-1} regions, corresponding to C═C vibration (Martins et al., 2013), became narrow after Pb^{2+} removal. The change of the peak shape might be due to the complexation of Pb^{2+} with C═C (π-electrons) band (Cao et al., 2009). As shown in Fig. 6, a new peak appeared at 1380 cm^{-1} after metal adsorption, suggesting the presence of surface carboxylic acid salts such as $Pb_3(CO_3)_2(OH)_2$ (Swiatkowski et al., 2004) or sulfuric acid salts such as $Pb(SO_4)\cdot PbO$ (Escalona Platero et al., 1996). This result was consistent with the XRD analyses (Fig. 5).

For the ferric-activated SBA, the bands at 580 and 481 cm^{-1} were assigned to the Fe—O bonds (Akbar et al., 2015; Tang et al., 2014). After the contact of Pb^{2+} ions with adsorbents, the peaks of Fe—O vibration at 580 and 481 cm^{-1} in the spectrum of ferric-activated SBA shifted to 575 and 466 cm^{-1}, respectively (Fig. 6). This shift denoted that the direct complexation between Pb^{2+} ions and iron compounds of adsorbent might be occurred. A similar observation was reported by Panda et al. (2011), and the shift of Fe—O band to lower wavenumber was caused by the adsorption of lead ions.

Table 5 Release of K^+, Na^+, $Ca^{2+}$and Mg^{2+} ions during removal process at initial pH 5.

Sample	The amount of released cations (mg/g)					Adsorption capacity (mg/g)
	$K^+/2$	$Na^+/2$	Ca^{2+}	Mg^{2+}	Sum	
SBA	0.51 ± 0.01	0.35 ± 0.03	1.36 ± 0.04	2.37 ± 0.02	4.59 ± 0.05	33.07 ± 0.02
Ferric-activated SBA	1.42 ± 0.02	0.98 ± 0.06	5.46 ± 0.01	1.11 ± 0.02	8.98 ± 0.06	42.66 ± 0.02

Please cite this article in press as: Yang, X. et al., Removal of lead from aqueous solutions by ferric activated sludge-based adsorbent derived from biological sludge. Arabian Journal of Chemistry (2016), http://dx.doi.org/10.1016/j.arabjc.2016.04.017

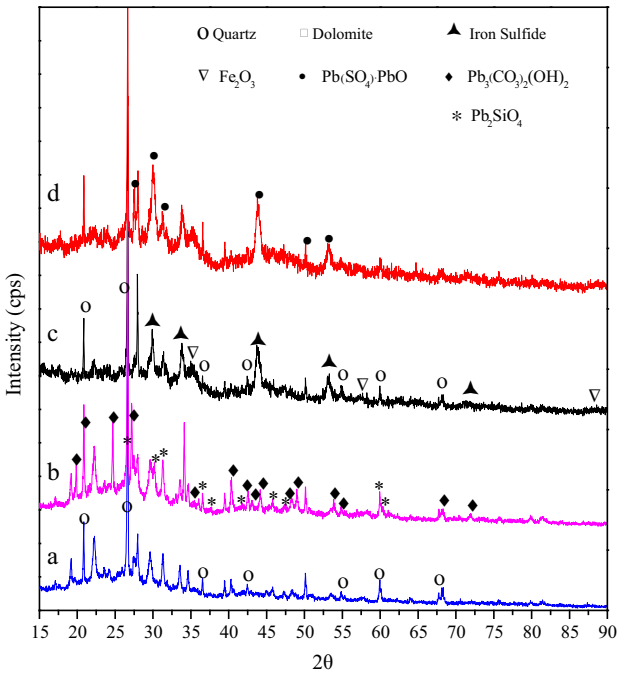

Figure 5 XRD patterns of SBA (a), Pb-loaded SBA (b), ferric-activated SBA (c), and Pb-loaded ferric activated SBA (d).

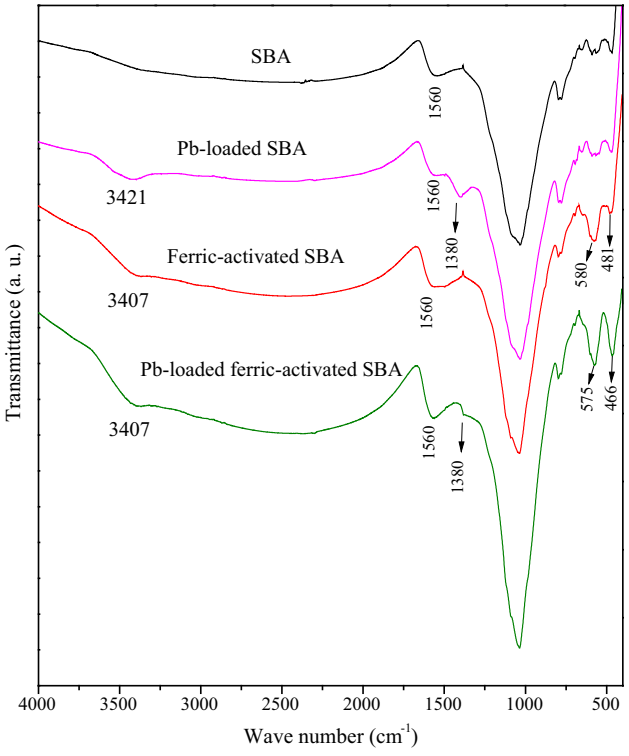

Figure 6 FTIR spectra of adsorbents before and after Pb^{2+} adsorption.

The iron oxides in the ferric-activated SBA were hydrolyzed to surface hydroxide groups that could react with Pb^{2+} ions to form metal-complex ($\equiv FeOPb^+$) (Stumm and Morgan, 1996). The formation of Fe—O—Pb structure was also reported by Zhang et al. (2013), using zerovalent iron nanoparticles for Pb(II) removal.

The higher adsorption capacity of ferric-activated SBA was due to the formation of the surface complex Fe—OPb^+ created by the reaction of Pb^{2+} ions and the hydrous oxide surface group Fe—OH, the precipitation, and the enhanced surface area after ferric activation that provide a larger number of active sites for Pb^{2+} ions.

In conclusion, the mechanism of Pb^{2+} adsorption on the SBA is a complex process, and encompasses the following: (a) Pb^{2+} adsorption via ion exchange with K^+, Na^+, Ca^{2+} and Mg^{2+}; (b) surface complexation; and (c) chemical precipitation. However, many factors can influence these mechanisms, such as pH, temperature, ionic strength, and concentration. Thus, details of the process and valuable quantitative information on the Pb^{2+} removal mechanisms need to be obtained by more in-depth research.

4. Conclusion

In this study, biological sludge was used as a low-cost feedstock to prepare adsorbents through ferric activation for the removal of Pb^{2+} ions. The results indicated that ferric-activated SBA showed a well-developed pore structure and enhanced Pb^{2+} adsorption ability, with an adsorption capacity of 42.96 mg/g. The adsorption of Pb^{2+} ions fitted well with the Freundlich isotherm, and the equilibrium kinetics agreed well with Pseudo-second order model. The mechanism of Pb^{2+} ions removal by the adsorbents involved ion exchange, precipitation, and surface complexation. The increased surface area and iron compounds of ferric-activated SBA promoted the removal of Pb^{2+} ions. Ferric-activated SBA produced from biological sludge could be used for removing Pb^{2+} ions from water, and it was beneficial to sludge reuse.

Acknowledgments

The authors gratefully acknowledge financial support from the National High Technology Research and Development Program of China (2012AA063508), Key Program of the National Natural Science Foundation of China (51038003), and National High Technology Research and Development Program of China (2011AA060906).

References

Ahmed, M.B., Zhou, J.L., Ngo, H.H., Guo, W., 2016. Insight into biochar properties and its cost analysis. Biomass Bioenergy 84, 76–86.

Akbar, A., Riaz, S., Ashraf, R., Naseem, S., 2015. Magnetic and magnetization properties of iron oxide thin films by microwave assisted sol-gel route. J. Sol–Gel Sci. Technol. 74, 320–328.

Babić, B.M., Milonjić, S.K., Polovina, M.J., Kaludierović, B.V., 1999. Point of zero charge and intrinsic equilibrium constants of activated carbon cloth. Carbon 37, 477–481.

Badruddoza, A.Z.M., Shawon, Z.B.Z., Tay, W.J.D., Hidajat, K., Uddin, M.S., 2013. Fe_3O_4/cyclodextrin polymer nanocomposites for selective heavy metals removal from industrial wastewater. Carbohyd. Polym. 91, 322–332.

Barrett, E.P., Joyner, L.G., Halenda, P.P., 1951. The determination of pore volume and area distributions in porous substances. I. Computations from nitrogen isotherms. J. Am. Chem. Soc. 73, 373–380.

Brunauer, S., Emmett, P.H., Teller, E., 1938. Adsorption of gases in multimolecular layers. J. Am. Chem. Soc. 60, 309–319.

Cao, X., Harris, W., 2010. Properties of dairy-manure-derived biochar pertinent to its potential use in remediation. Bioresour. Technol. 101, 5222–5228.

Cao, X., Ma, L., Gao, B., Harris, W., 2009. Dairy-manure derived biochar effectively sorbs lead and atrazine. Environ. Sci. Technol. 43, 3285–3291.

Chen, T., Zhang, Y., Wang, H., Lu, W., Zhou, Z., Zhang, Y., Ren, L., 2014. Influence of pyrolysis temperature on characteristics and heavy metal adsorptive performance of biochar derived from municipal sewage sludge. Bioresour. Technol. 164, 47–54.

Elaigwu, S.E., Rocher, V., Kyriakou, G., Greenway, G.M., 2014. Removal of Pb^{2+} and Cd^{2+} from aqueous solution using chars from pyrolysis and microwave-assisted hydrothermal carbonization of *Prosopis africana* shell. J. Ind. Eng. Chem. 20, 3467–3473.

Escalona Platero, E., Pe Arroya Mentruit, M., Otero Areán, C., Zecchina, A., 1996. FTIR studies on the acidity of sulfated zirconia prepared by thermolysis of zirconium sulfate. J. Catal. 162, 268–276.

Ge, F., Li, M., Ye, H., Zhao, B., 2012. Effective removal of heavy metal ions Cd^{2+}, Zn^{2+}, Pb^{2+}, Cu^{2+} from aqueous solution by polymer-modified magnetic nanoparticles. J. Hazard. Mater. 211–212, 366–372.

Hadi, P., Xu, M., Ning, C., Sze Ki Lin, C., McKay, G., 2015. A critical review on preparation, characterization and utilization of sludge-derived activated carbons for wastewater treatment. Chem. Eng. J. 260, 895–906.

Hien Hoa, T.T., Liamleam, W., Annachhatre, A.P., 2007. Lead removal through biological sulfate reduction process. Bioresour. Technol. 98, 2538–2548.

Ihsanullah, Abbas, A., Al-Amer, A.M., Laoui, T., Al-Marri, M.J., Nasser, M.S., Khraisheh, M., Atieh, M.A., 2016. Heavy metal removal from aqueous solution by advanced carbon nanotubes: critical review of adsorption applications. Sep. Purif. Technol. 157, 141–161.

Iqbal, M., Saeed, A., Zafar, S.I., 2009. FTIR spectrophotometry, kinetics and adsorption isotherms modeling, ion exchange, and EDX analysis for understanding the mechanism of Cd^{2+} and Pb^{2+} removal by mango peel waste. J. Hazard. Mater. 164, 161–171.

Jin, H., Capareda, S., Chang, Z., Gao, J., Xu, Y., Zhang, J., 2014. Biochar pyrolytically produced from municipal solid wastes for aqueous As(V) removal: adsorption property and its improvement with KOH activation. Bioresour. Technol. 169, 622–629.

Kacan, E., 2016. Optimum BET surface areas for activated carbon produced from textile sewage sludges and its application as dye removal. J. Environ. Manage. 166, 116–123.

Karami, H., 2013. Heavy metal removal from water by magnetite nanorods. Chem. Eng. J. 219, 209–216.

Li, W., Gong, X., Li, X., Zhang, D., Gong, H., 2012. Removal of Cr (VI) from low-temperature micro-polluted surface water by tannic acid immobilized powdered activated carbon. Bioresour. Technol. 113, 106–113.

Liu, C., Tang, Z., Chen, Y., Su, S., Jiang, W., 2010. Characterization of mesoporous activated carbons prepared by pyrolysis of sewage sludge with pyrolusite. Bioresour. Technol. 101, 1097–1101.

Lu, H., Zhang, W., Yang, Y., Huang, X., Wang, S., Qiu, R., 2012. Relative distribution of Pb^{2+} sorption mechanisms by sludge-derived biochar. Water Res. 46, 854–862.

Martins, A.E., Pereira, M.S., Jorgetto, A.O., Martines, M.A.U., Silva, R.I.V., Saeki, M.J., Castro, G.R., 2013. The reactive surface of Castor leaf [*Ricinus communis* L.] powder as a green adsorbent for the removal of heavy metals from natural river water. Appl. Surf. Sci. 276, 24–30.

Méndez, A., Terradillos, M., Gascó, G., 2013. Physicochemical and agronomic properties of biochar from sewage sludge pyrolysed at different temperatures. J. Anal. Appl. Pyrol. 102, 124–130.

Mohan, D., Kumar, H., Sarswat, A., Alexandre-Franco, M., Pittman, C.U., 2014. Cadmium and lead remediation using magnetic oak wood and oak bark fast pyrolysis bio-chars. Chem. Eng. J. 236, 513–528.

Nguyen, T.A.H., Ngo, H.H., Guo, W.S., Zhang, J., Liang, S., Yue, Q. Y., Li, Q., Nguyen, T.V., 2013. Applicability of agricultural waste and by-products for adsorptive removal of heavy metals from wastewater. Bioresour. Technol. 148, 574–585.

Pan, Z., Tian, J., Xu, G., Li, J., Li, G., 2011. Characteristics of adsorbents made from biological, chemical and hybrid sludges and their effect on organics removal in wastewater treatment. Water Res. 45, 819–827.

Panda, L., Das, B., Rao, D.S., 2011. Studies on removal of lead ions from aqueous solutions using iron ore slimes as adsorbent. Korean J. Chem. Eng. 28, 2024–2032.

Rio, S., Faur-Brasquet, C., Le Coq, L., Le Cloirec, P., 2005. Structure characterization and adsorption properties of pyrolyzed sewage sludge. Environ. Sci. Technol. 39, 4249–4257.

Stumm, W., Morgan, J.J., 1996. Aquatic Chemistry, third ed. Wiley-Interscience, New York, p. 572.

Sud, D., Mahajan, G., Kaur, M.P., 2008. Agricultural waste material as potential adsorbent for sequestering heavy metal ions from aqueous solutions – a review. Bioresour. Technol. 99, 6017–6027.

Swiatkowski, A., Pakula, M., Biniak, S., Walczyk, M., 2004. Influence of the surface chemistry of modified activated carbon on its electrochemical behaviour in the presence of lead(II) ions. Carbon 42, 3057–3069.

Tang, L., Yang, G., Zeng, G., Cai, Y., Li, S., Zhou, Y., Pang, Y., Liu, Y., Zhang, Y., Luna, B., 2014. Synergistic effect of iron doped ordered mesoporous carbon on adsorption-coupled reduction of hexavalent chromium and the relative mechanism study. Chem. Eng. J. 239, 114–122.

Trakal, L., Šigut, R., Šillerová, H., Faturíková, D., Komárek, M., 2014. Copper removal from aqueous solution using biochar: effect of chemical activation. Arabian J. Chem. 7, 43–52.

Velghe, I., Carleer, R., Yperman, J., Schreurs, S., D'Haen, J., 2012. Characterisation of adsorbents prepared by pyrolysis of sludge and sludge/disposal filter cake mix. Water Res. 46, 2783–2794.

Wang, F.Y., Wang, H., Ma, J.W., 2010. Adsorption of cadmium (II) ions from aqueous solution by a new low-cost adsorbent-Bamboo charcoal. J. Hazard. Mater. 177, 300–306.

Wang, Z., Liu, G., Zheng, H., Li, F., Ngo, H.H., Guo, W., Liu, C., Chen, L., Xing, B., 2015. Investigating the mechanisms of biochar's removal of lead from solution. Bioresour. Technol. 177, 308–317.

Xu, G., Yang, X., Spinosa, L., 2015. Development of sludge-based adsorbents: preparation, characterization, utilization and its feasibility assessment. J. Environ. Manage. 151, 221–232.

Xu, G., Zhang, W., Li, G., 2005. Adsorbent obtained from CEPT sludge in wastewater chemically enhanced treatment. Water Res., 5175–5185

Yang, X., Xu, G., Yu, H., Zhang, Z., 2016. Preparation of ferric-activated sludge-based adsorbent from biological sludge for tetracycline removal. Bioresour. Technol. 211, 566–573.

Yu, X., Tong, S., Ge, M., Wu, L., Zuo, J., Cao, C., Song, W., 2013. Adsorption of heavy metal ions from aqueous solution by carboxylated cellulose nanocrystals. J. Environ. Sci. 25, 933–943.

Zhang, Y., Su, Y., Zhou, X., Dai, C., Keller, A.A., 2013. A new insight on the core-shell structure of zerovalent iron nanoparticles and its application for Pb(II) sequestration. J. Hazard. Mater. 263, 685–693.

Zhu, W., Sun, S., Gao, J., Fu, F., Chung, T., 2014. Dual-layer polybenzimidazole/polyethersulfone (PBI/PES) nanofiltration (NF) hollow fiber membranes for heavy metals removal from wastewater. J. Membr. Sci. 456, 117–127.

Zhu, Z., Gao, C., Wu, Y., Sun, L., Huang, X., Ran, W., Shen, Q., 2013. Removal of heavy metals from aqueous solution by lipopeptides and lipopeptides modified Na-montmorillonite. Bioresour. Technol. 147, 378–386.

Zielińska, A., Oleszczuk, P., 2015. Evaluation of sewage sludge and slow pyrolyzed sewage sludge-derived biochar for adsorption of phenanthrene and pyrene. Bioresour. Technol. 192, 618–626.

Please cite this article in press as: Yang, X. et al., Removal of lead from aqueous solutions by ferric activated sludge-based adsorbent derived from biological sludge. Arabian Journal of Chemistry (2016), http://dx.doi.org/10.1016/j.arabjc.2016.04.017